Int. J. Plant Sci. 167(1):19–32. 2006.

1058-5893/2006/16701-0003$15.00

# SIZE-DEPENDENT VARIATION IN SHOOT LIGHT-HARVESTING EFFICIENCY IN SHADE-INTOLERANT CONIFERS

Ülo Niinemets,[1,*,†] Mari Tobias,* Alessandro Cescatti,† and Ashley Sparrow‡

*Department of Plant Physiology, Institute of Molecular and Cell Biology, University of Tartu, Riia 23, Tartu 51010, Estonia; †Centro di Ecologia Alpina, I-38040 Viote del Monte Bondone (TN), Italy; and ‡School of Biological Sciences, University of Canterbury, Private Bag 4800, Christchurch 8020, New Zealand

Shoots and foliage elements of shade-intolerant conifers strongly vary in size, but the effects of size on shoot light-harvesting efficiency have not been quantified. We investigated shoot adaptation to seasonal average integrated quantum flux density in gymnosperms *Pinus palustris* Mill., *P. patula* Schlect. & Cham., and *P. radiata* D. Don. and angiosperm *Casuarina glauca* Sieb. ex Spreng. In addition, *P. sylvestris* L., sampled from infertile and fertile sites, and *P. taeda* L. were included to test for general correlations among shoot architecture and size. All studied species possess needle-like photosynthetic elements. A shoot model was fitted to the data to separate the determinants of shoot light-harvesting efficiency. The model estimated shoot light harvesting on the basis of angular distribution of foliage surface areas, degree of spatial clumping, foliage area density in shoot volume, and beam path length in shoot volume. Increases in irradiance primarily led to greater foliage aggregation, greater foliage area density in shoot volume, and to a minor degree, to changes in foliage area angular distribution. Greater foliage aggregation resulted in lower efficiency of light harvesting but greater investment of foliar biomass in high light where the photosynthetic returns are greater. The species behave similarly except that the light-harvesting characteristics of *P. patula*, which has long, strongly bending needles, were independent of light. In all species, the shoots were larger in higher irradiance, and the fraction of biomass in shoot axis increased with increasing irradiance, indicating greater costs for light harvesting in high light. There were further significant species differences in light-harvesting efficiency that were linked to differences in foliage and shoot size. Foliage element length varied between 1.1 and 31.4 cm and shoot axis length between 1.2 and 36.5 cm among the species, leading to 4 orders of magnitude variation in shoot cylinder volume and three orders of magnitude variation in foliage area density ($\rho$); $\rho$ decreased with increasing foliage element length and shoot volume. The degree of foliage clumping scaled positively with $\rho$ and negatively with foliage element length. Foliage clumping was positively associated with foliage dry mass to shoot silhouette area ratio, signifying a trade-off between efficient light harvesting and large photosynthetic biomass accumulation. These data demonstrate a general increase of light-harvesting efficiency with increasing length of foliage elements, but they also demonstrate that this increase is limited by enhanced bending of longer foliage elements and by augmented support costs.

*Keywords:* foliage aggregation, foliage length, interspecific variability, light harvesting, support costs.

## Introduction

Plant structure strongly adapts to long-term light conditions to increase light-harvesting efficiency in low light and light-use efficiency in high light (Valladares 2003; Pearcy et al. 2005; Niinemets and Sack 2006). Such structural modifications to local light environment constitute the primary means to enhance the whole-canopy light capture and use efficiency.

In conifers, decreases in light availability from canopy top to bottom result in increases in shoot silhouette to total area ratio, thereby enhancing the light-harvesting efficiency of unit foliage area (Stenberg et al. 1998, 1999, 2001; Niinemets et al. 2002*a*; Cescatti and Zorer 2003). Changes in shoot light-harvesting efficiency can result from different combinations of foliage dispersion, distribution of foliage area inclination angles, and foliage area density (Niinemets et al. 2002*a*; Cescatti and Zorer 2003; Cescatti and Niinemets 2004), but the limits of and controls on specific acclimation responses in shoot architecture are not fully understood.

In some species, irradiance affects both foliage surface angular distributions and aggregation (Cescatti and Zorer 2003), but in other species light affects more strongly either foliage spatial clumping (Niinemets et al. 2002*a*) or angular distributions (Niinemets et al. 2004). While in broad-leaved species various architectural attributes may lead to convergent light-harvesting efficiency (Valladares et al. 2000, 2002; Niinemets et al. 2004), conifer species differ in the efficiency of and plastic modifications in light-harvesting efficiency (Stenberg et al. 1998, 1999, 2001; Niinemets et al. 2002*a*; Cescatti and Zorer 2003; Cescatti and Niinemets 2004).

This extensive variation in conifer light-harvesting efficiency may be linked partly to species differences in the size

[1] Author for correspondence; fax 00372-7-366021; e-mail ylon@ut.ee.

*Manuscript received March 2005; revised manuscript received August 2005.*

of foliage elements and the size of shoots. Self-shading within the shoot can be minimized effectively by increasing the distance of foliage elements from the point of attachment to the stem (Takenaka 1994; Pearcy and Yang 1998), suggesting that light-harvesting efficiency increases with increasing the length of foliage elements. However, more light penetrates the canopies of pine species with long, bending needles than the canopies of conifers with shorter, rigid needles (Battaglia 2000; Yirdaw and Luukkanen 2004). As the costs for foliage support increase with the cube of the length of foliage elements (Niklas 1991), increases in length may lead to greater aggregation of foliage elements and to inefficient leaf angle distribution because of support limitations. Thus, enhanced support costs may constrain length-dependent increases in shoot light-harvesting efficiency.

Apart from modification of light interception, augmented foliage aggregation in high light results in accumulation of foliage biomass per unit shoot silhouette area (Niinemets et al. 2002*a*; Cescatti and Zorer 2003). Thus, a greater degree of foliage clumping in high irradiance leads to investment of foliage biomass where the shoot potential photosynthetic production is the largest, thereby maximizing canopy photosynthesis for a given biomass in foliage. This implies that light- and species-dependent changes in shoot architecture not only may be driven by the requirements for efficient light harvesting but also may reflect the fundamental compromise between efficient light harvesting and use in photosynthesis. While light harvesting per unit leaf area is maximized when there is no self-shading within the shoot, light saturation of needle photosynthesis occurs below full sunlight. Thus, in high-light-exposed conifer shoots, whole shoot photosynthesis is maximized when there is a certain degree of foliage clumping within the shoot.

We studied shoot acclimation to long-term light availability in four conifers of contrasting foliage element length to determine the relative importance of light-dependent variations in angular distribution of foliage surface area, spatial clumping, and foliage area density on shoot light-harvesting efficiency in species with varying length and stiffness of foliage elements. *Pinus palustris* Mill., *P. patula* Schlect. & Cham., and *P. radiata* D. Don. are gymnosperm conifers, while *Casuarina glauca* Sieb. ex Spreng. is a cone-bearing angiosperm. We further tested for a general hypothesis of a negative scaling of foliage area density and foliage aggregation with the length of foliage elements in an extended data set including these four species and *P. taeda* L. and *P. sylvestris* L. (Niinemets et al. 2002*a*). With this extended data set we also tested the hypothesis of a universal trade-off between efficient light harvesting and enhanced photosynthetic potential.

## Methods

### *Study Species*

All studied species are intolerant to shade. *Pinus palustris* and *P. taeda* are widespread species in North American warm temperate to subtropical forests. Both species can grow on nutrient-poor soils with moderate to excessive drainage. *Pinus palustris* may form mixed stands with *P. taeda* on especially poor sites, but it grows best in complete absence of competition (Boyer 1990). *Pinus palustris* can only survive in natural open savanna-like stands on nutrient-poor soils where ground fires that control understory vegetation and soil organic matter content regularly occur (Platt et al. 1988; Harcombe et al. 1993).

*Pinus radiata* is a rare species in its native habit in the coastal fog belt in California and Baja California. It has a shallow root system and requires deep, medium-textured soils for best performance (Burns and Honkala 1990; Immel 2002). Although of limited dispersal in natural sites, *P. radiata* is the most widely planted pine species in the temperate oceanic, Mediterranean, and subtropical Southern Hemisphere (Richardson 1998; Immel 2002).

*Pinus patula* is native in the Sierra Madre Oriental in Mexico (Perry 1991; Richardson and Rundel 1998) but is widely planted in warm temperate, Mediterranean, subtropical, and tropical lowland forests as well as in humid mountain and dry afromontane forests because of fast growth rate (Richardson 1998; Verzino et al. 1999; Immel 2002; van Wesenbeeck et al. 2003). *Pinus patula* forms relatively open stands in plantations and naturalized sites (Lemeniha et al. 2004; Yirdaw and Luukkanen 2004). It tolerates lower water availabilities but requires higher minimum temperatures than *P. radiata* (Richardson 1998).

*Casuarina glauca* is a cone-bearing angiosperm native to tropical and temperate coasts of eastern Australia (Wilson and Johnson 1989). It can colonize poor soils because of nitrogen-fixing capacity, and, because of high salinity tolerance, it

**Table 1**

**Foliage Element Length, Shoot Axis Length, Number of Foliage Elements on Shoot, and Number of Shoots Sampled for Six Conifer Species**

| | Foliage element length (cm) | | Shoot axis length (cm) | | Number of foliage elements on shoot | | |
|---|---|---|---|---|---|---|---|
| Species | Range | Average ± SE | Range | Average ± SE | Range | Average ± SE | Number of shoots sampled |
| *Casuarina glauca* | 9.6–31.4 | 20.2 ± 1.0 | 7.5–30.5 | 14.2 ± 1.2 | 19–147 | 68 ± 7 | 25 |
| *Pinus palustris* | 22.8–30.4 | 27.9 ± 0.9 | 4.9–23.1 | 10.1 ± 2.4 | 93–783 | 482 ± 84 | 8 |
| *P. patula* | 19.1–29.2 | 25 ± 5 | 2.5–33.5 | 15.3 ± 2.1 | 56–523 | 277 ± 30 | 20 |
| *P. radiata* | 10.0–16.6 | 14.2 ± 4.3 | 4.3–31.3 | 16.5 ± 1.6 | 59–557 | 336 ± 27 | 20 |
| *P. sylvestris* (fertile) | 2.5–7.3 | 5.10 ± 0.12 | 1.6–36.5 | 9.4 ± 1.0 | 10–622 | 122 ± 17 | 52 |
| *P. sylvestris* (infertile) | 1.1–5.9 | 2.46 ± 0.73 | 1.2–8.0 | 3.3 ± 1.5 | 29–194 | 93.8 ± 3.4 | 90 |
| *P. taeda* | 11.9–15.0 | 13.5 ± 0.9 | 15.5–29.2 | 20.2 ± 4.5 | 141–363 | 240 ± 65 | 3 |

Source. The data for *P. sylvestris* were reported by Niinemets et al. (2002*a*).

often grows in monospecific stands in sites with shallow saline groundwater along estuaries and streams (Wilson and Johnson 1989). *Casuarina* species have been introduced to many tropical and subtropical countries for stabilization of sand dunes and biomass production as well as for improvement of soils (Dutta and Agrawal 2001; Warren and Zou 2002; Rajendran and Devaraj 2004). Because of fast growth rates and strong competitive potentials in stressful environments, *C. glauca*, *P. patula*, and *P. radiata* are strong invasives in many countries (Langeland and Craddock Burks 1998; Richardson 1998; Immel 2002).

*Pinus sylvestris* is one of the most widely dispersed and competitive conifers in Eurasia. It inhabits sites with strongly varying nutrient and water availabilities (Linder 1987), but growth in poor sites leads to distinct modifications in needle, shoot, and crown architecture (Niinemets et al. 2001, 2002*a*).

*Casuarina glauca*, *P. palustris*, and *P. patula* are the species with the longest foliage elements, and *P. sylvestris* is the species with the shortest needles, in particular, in the infertile sites (table 1). In *P. palustris*, *P. patula*, *P. radiata*, and *P. taeda*, the needles are in fascicles of three with the shape of needle cross-section approximating a sector of a circle, while the two-needled fascicles of *P. sylvestris* have needles with hemicircular to hemielliptical cross-section, and the cladodes of *C. glauca* are circular. Among the species with the longest foliage elements, *C. glauca* has the thickest foliage (average ± SE cladode diameter = 1.431 ± 0.043 mm), followed by *P. palustris* (average needle thickness ± SE = 0.88 ± 0.06 mm) and *P. patula* (average thickness = 0.612 ± 0.018 mm). Because of low thickness and large length, the needles of *P. patula* are soft and strongly bend on the shoot under the needle's own weight (fig. 1). Shoots of *C. glauca* are the most sparsely foliated (table 1).

### *Study Sites*

*Pinus palustris* and *P. taeda* were sampled in the Southeast Tree Research and Education Site (SETRES), Carolina Sandhills, Scotland County, North Carolina (34°55′N, 79°30′W), in the beginning of December 1998. The stand was on poor, excessively drained soil and was dominated by *P. taeda* (density 1260 stems $ha^{-1}$) that had been planted after harvesting of a 65-yr-old forest of *P. palustris*. In addition to *P. taeda*,

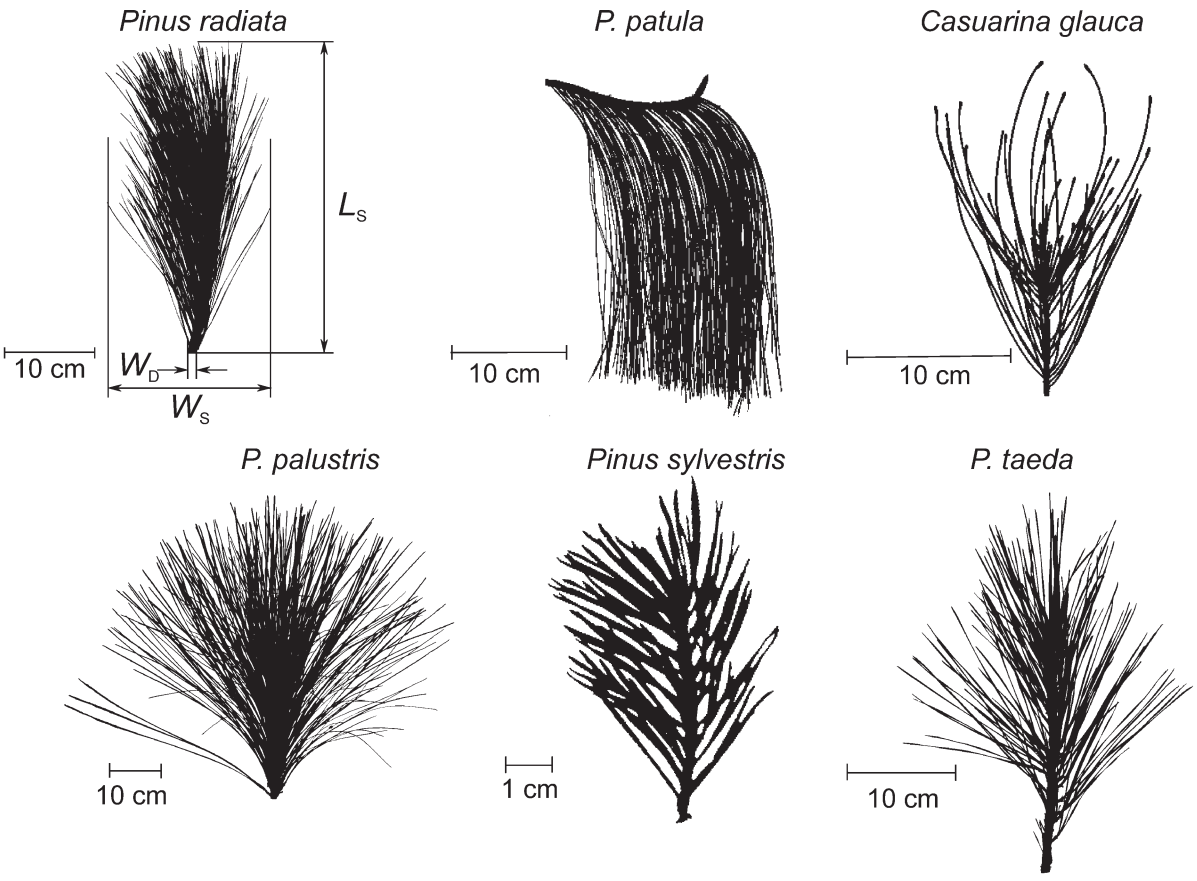


**Fig. 1** Representative shoot silhouettes (projection 0°, 0°, i.e., the upper face of the shoot perpendicular to the view direction) of the studied conifers and illustration of measurements of shoot length ($L_S$), shoot width ($W_S$), and shoot axis width ($W_D$). All studied species are gymnosperms except for *Casuarina glauca*, which is a cone-bearing angiosperm. The shoots depicted were taken from midcanopy and had been exposed to seasonal average daily integrated quantum flux densities of 18.6 mol $m^{-2}$ $d^{-1}$ (*C. glauca*), 19.2 mol $m^{-2}$ $d^{-1}$ (*Pinus palustris*), 17.2 mol $m^{-2}$ $d^{-1}$ (*P. patula*), 15.0 mol $m^{-2}$ $d^{-1}$ (*P. radiata*), 16.3 mol $m^{-2}$ $d^{-1}$ (*P. sylvestris*, infertile site), and 19.8 mol $m^{-2}$ $d^{-1}$ (*P. taeda*). Ranges and averages of foliage element and shoot lengths are provided in table 1.

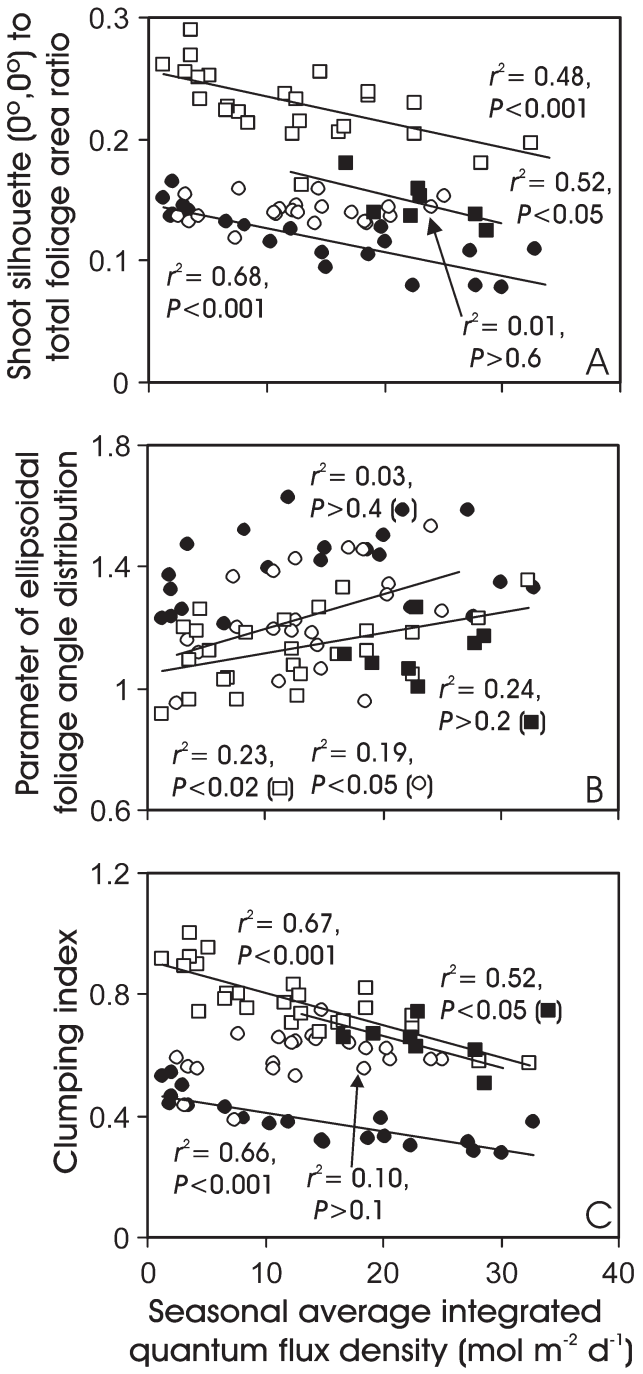


**Fig. 2** Effects of seasonal average integrated quantum flux density on shoot silhouette (projection 0°, 0°; fig. 1) to total area ratio (*A*), parameter of the ellipsoidal distribution of foliage surface area (*B*; *c* in eqq. [4], [5]), and the clumping index (*C*; $\lambda_0$; eq. [2]) in *Casuarina glauca* (open squares), *Pinus palustris* (filled squares), *P. patula* (open circles), and *P. radiata* (filled circles). Leaf surface area is spherically distributed if $c = 1$, while $c > 1$ for horizontal distributions and $c < 1$ for vertical distributions. Leaf clumping index (eq. [2]) characterizes the degree of departure of spatial dispersion of foliage elements from a random dispersion ($\lambda_0 = 1$). Foliage becomes more aggregated and intercepts less irradiance with decreasing $\lambda_0$. Data were fitted by linear regressions. The values of *c* rely on a different set of shoot projections in *P. patula* (see "Methods") and are, therefore, not directly comparable with those in the other species. Nevertheless, *c* values were consistently determined for all shoots for this species and are, therefore, still illustrative of the overall trends in needle angular distribution with canopy light environment.

a few naturally seeded individuals of *P. palustris* were present at the site. A fertilization and irrigation experiment had been launched at the site in 1992 (Murthy and Dougherty 1997; Dougherty et al. 1998), but we sampled foliage only from the control plots. The sampled trees were 7–9 m tall and 16 yr old. Further details of this site are provided in an earlier study (Niinemets et al. 2002*b*).

*Casuarina glauca*, *P. patula*, and *P. radiata* were studied on the campus of the University of Canterbury, Christchurch, South Island, New Zealand (43°32′S, 172°35′E, elevation 20 m), in the beginning of April 2002. Two mature male and two female *C. glauca* trees (height 17.8–19 m, circumference at breast height 0.31–0.46 m) were chosen for the study. The selected trees were partly shaded by other neighboring *Casuarina* trees and natural woody vegetation growing on the campus. *Casuarina glauca* is an exotic species in New Zealand, but it is one of the *Casuarina* species with northernmost native distribution along the east coast of Australia. It is a vigorous invasive species in New Zealand that spreads in the coastal regions with mild maritime climate, reaching its potential maximum height of 20 m in 8–15 yr (Niinemets et al. 2005*a*).

Two mature trees of *P. patula* (height 20.5 and 21.1 m, circumference at breast height 0.74 and 0.91 m) and two mature trees of *P. radiata* (height 13.5 and 16.0, circumference 0.32 and 0.54 m) were sampled. Partial shading of the study trees was provided by adjacent *P. patula*, *P. pinea*, and *P. pinaster* trees. These introduced species are widely used in forest plantations, with *P. radiata* being the most important forestry species in New Zealand. Both *P. patula* and *P. radiata* have fast growth rates in the temperate oceanic climate.

The data of *P. sylvestris* reported by Niinemets et al. (2002*a*) were also included to enhance the generality of correlations between shoot structure and light interception. Three trees in this data set were selected in a fertile site on mineral soil in Ahunapalu, Estonia (stand density 1200 trees ha$^{-1}$; 58°19′N, 27°17′E, elevation ca. 60 m above sea level), and 22 trees were sampled in the infertile site on thick peat in Männikjärve raised bog, Endla State Nature Reserve, Estonia (stand density 200 trees ha$^{-1}$; 58°52′N, 26°13′E, elevation 5–30 m above sea level). The samples were taken in August–October 1998 and 1999. Previous analyses demonstrated that the needles were shorter (table 1; Niinemets et al. 2001) and more strongly clumped in the infertile site (Niinemets et al. 2002*a*). Detailed description of this site and the measurement protocols are provided in Niinemets et al. (2002*a*).

### *Shoot Sampling*

Terminal shoots with all current-year needles were sampled in pines. In *Casuarina*, the main photosynthetic organs are first-order throwaway cladodes (Wilson and Johnson 1989;

Berg 1994), and terminal branchlets with all current-year first-order cladodes were sampled in this species. In all cases, the shoots were sampled from canopy top to bottom within the natural light gradient in the canopy.

Shoot inclination angle with respect to the horizontal was measured *in situ* with a protractor and plumb line, and shoot azimuth angle was measured by a compass with magnetic north correction. The sampled shoots were put in plastic bags with wet filter paper and taken immediately to the laboratory for morphological measurements. The sizes of shoots, number of foliage elements on the shoots, and total number of shoots taken are reported in table 1.

### *Long-Term Shoot Light Environment*

Shoot long-term light environment was characterized by hemispherical photographs that were taken above every shoot before harvesting. At the North Carolina site, we used a Nikon camera equipped with Nikkor 8-mm fish-eye f/8 lens and a high-resolution slide film, as detailed by Niinemets et al. (2002*b*). In New Zealand, we employed a Nikon Coolpix 990 digital camera equipped with a Nikon Fisheye Converter FC-E8 ×0.21.

The slides taken with the film camera were digitized with FilmScan 200 (Epson Europe, Amsterdam, Netherlands) with a resolution of 1200 dpi. The digital RGB (red/green/blue) color images were converted to black-and-white in two steps to improve the repeatability. First, the 24-bit image was converted to gray-tone bitmaps corresponding to each color channel (red/green/blue) by Corel Photopaint 8.369 software. For black-and-white conversion (1-bit image), we selected the gray-tone bitmap of the blue channel, in which the leaves are essentially black. WinPhot 5.0 software (ter Steege 1996) was used to determine the fraction of diffuse light of open sky (diffuse site factor, $I_D$) and the fraction of potential penetrating direct light of open sky (direct site factor, $I_B$) from the 1-bit images. Hale and Edwards 2002, using the same film and digital cameras, demonstrated that film and digital photographic techniques provide matching estimates of canopy light climate.

Average seasonal daily integrated photosynthetically active quantum flux densities ($Q_{int}$, mol $m^{-2}$ $d^{-1}$) were determined for the period April 1–October 31, 1998, for the North Carolina site, and for November 1, 2001–February 28, 2002, for the New Zealand site. In both sites, these are the periods of foliage growth and development. The fractional contributions of diffuse irradiance during this period were 0.60 for the North Carolina site (Niinemets et al. 2002*b*) and 0.53 for the New Zealand site (Niinemets et al. 2005*b*). To convert the relative light measures provided by hemispherical photography to $Q_{int}$, we used direct measurements of quantum flux density with quantum sensors in the North Carolina site (Ellsworth 2000), while the daily values of above-canopy global solar radiation ($R_G$, MJ $m^{-2}$ $d^{-1}$) measured in Christchurch (unpublished data of the Department of Geography, University of Canterbury) were employed for the New Zealand site as described by Niinemets et al. (2005*b*). These measurements provided an average integrated above-canopy quantum flux density of 43.0 mol $m^{-2}$ $d^{-1}$ for the North Carolina site and 36.0 mol $m^{-2}$ $d^{-1}$ for the New Zealand site (Niinemets et al. 2002*b*, 2005*b*).

### *Shoot and Foliage Element Measurements*

For shoot silhouette images, the shoots were placed in front of a white projection screen in a dark room, and the screen was backlit by two overhead projectors arranged to produce a completely uniform radiation field. Shoot photographs were taken from a distance of 5 m. A Nikon film camera with a 180-mm Nikkor tele-lens was used for the shoots of *P. palustris* and *P. taeda*, while a Nikon Coolpix 990 camera with Tele Converter TC-E2 ×2 was used for *C. glauca*, *P. patula*, and *P. radiata*. Objects of known size were photographed together with the shoots for calibration.

The shoot silhouettes were photographed under different view directions defined by shoot inclination ($\varphi$) and rotation angles ($\phi$). The shoot rotation angle is the angle of shoot rotation around its main axis (Stenberg et al. 1998), and the inclination angle is the angle of shoot axis relative to the projection plane. In general, the silhouettes ($\phi, \varphi$) measured were (0°, 0°), (45°, 0°), (90°, 0°), (0°, 45°), and (0°, 90°). The projection (0°, 0°), for which the upper face of the shoot is perpendicular to the view direction (fig. 1), generally provides the largest shoot silhouette area. For the projection (45°, 0°) the shoot is rotated 45° around its axis, while it is rotated 90° for the projection (90°, 0°). The shoot is inclined by 45° relative to horizontal for the projection (0°, 45°), and the projection (0°, 90°) is the shoot axial view. These projections provide a realistic description of shoot light-harvesting efficiency (Cescatti and Zorer 2003). For *P. palustris* and *P. taeda*, we determined silhouettes (0°, 0°) and (90°, 0°) that provide the minimum required to parameterize the shoot radiative transfer model (Niinemets et al. 2002*a*; Cescatti and Zorer 2003).

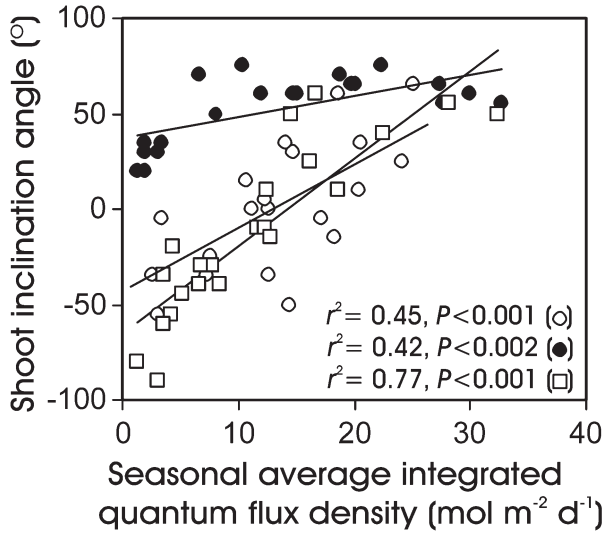


**Fig. 3** Relationships between $Q_{int}$ and shoot inclination angle relative to horizontal in *Casuarina glauca*, *Pinus patula*, and *P. radiata*. Symbols as in fig. 2. Data were fitted by linear regressions.

The projections $(0°, 0°)$, $(45°, 0°)$, and $(90°, 0°)$ initially were made for the shoot axis arranged vertically. However, *C. glauca* had slightly bending foliage, and *P. patula* had strongly bending foliage (fig. 1). To more realistically represent the shoot natural position and needle arrangement in the canopy for these species, we additionally determined the projections $(0°, 0°)$ and $(0°, 45°)$ for the shoot axis placed in a horizontal position (fig. 1). The projection $(0°, \varphi)$, with $\varphi$ set to the shoot inclination in the natural position in the canopy, also was made. For *C. glauca*, the silhouette areas of the equivalent projections with vertical and horizontal shoot axis were averaged before fitting the shoot model (see "Model Parameterization" below) to the data, while the projections with vertical shoot axis were discarded in *P. patula*.

The slides were scanned as with the hemispheric photographs, and the shoot silhouette areas, $A_S(\phi, \varphi)$, were estimated from all digital images by the UTHSCSA Imagetool 2.00alpha (C. Donald Wilcox, S. Brent Dove, W. Doss McDavid, and David B. Greer, Department of Dental Diagnostic Science, University of Texas Health Science Center, San Antonio, TX; http://ddsdx.uthscsa.edu). Because every image file was calibrated separately, a precision better than 2% was achieved in the area measurements.

Shoot projections with $\varphi = 0°$ were further employed to measure shoot length ($L_S$), and the projections $(0°, 0°)$ and $(0°, 90°)$ were used to measure shoot width ($W_S$), while shoot height ($H_S$) was measured from projections $(90°, 0°)$ and $(0°, 90°)$, and the volume of the shoot cylinder was calculated assuming an elliptical shoot cross-section (elliptical cylinder; Niinemets et al. 2002*a*; Cescatti and Zorer 2003). In *C. glauca* and *P. patula*, $L_S$ and $W_S$ were measured from shoot silhouettes determined for a horizontal shoot axis. The shoot foliage area density, $\rho$ ($cm^2\ cm^{-3}$), was further determined as

$$\rho = \frac{4A_L}{\pi H_S W_S L_S}, \quad (1)$$

where $A_L$ is half of the total foliage area. Half of the total area is commonly used in radiative transfer studies for objects of complex geometry because the mean projection coefficient of a randomly oriented convex solid is 0.5 (Chen and Black 1992).

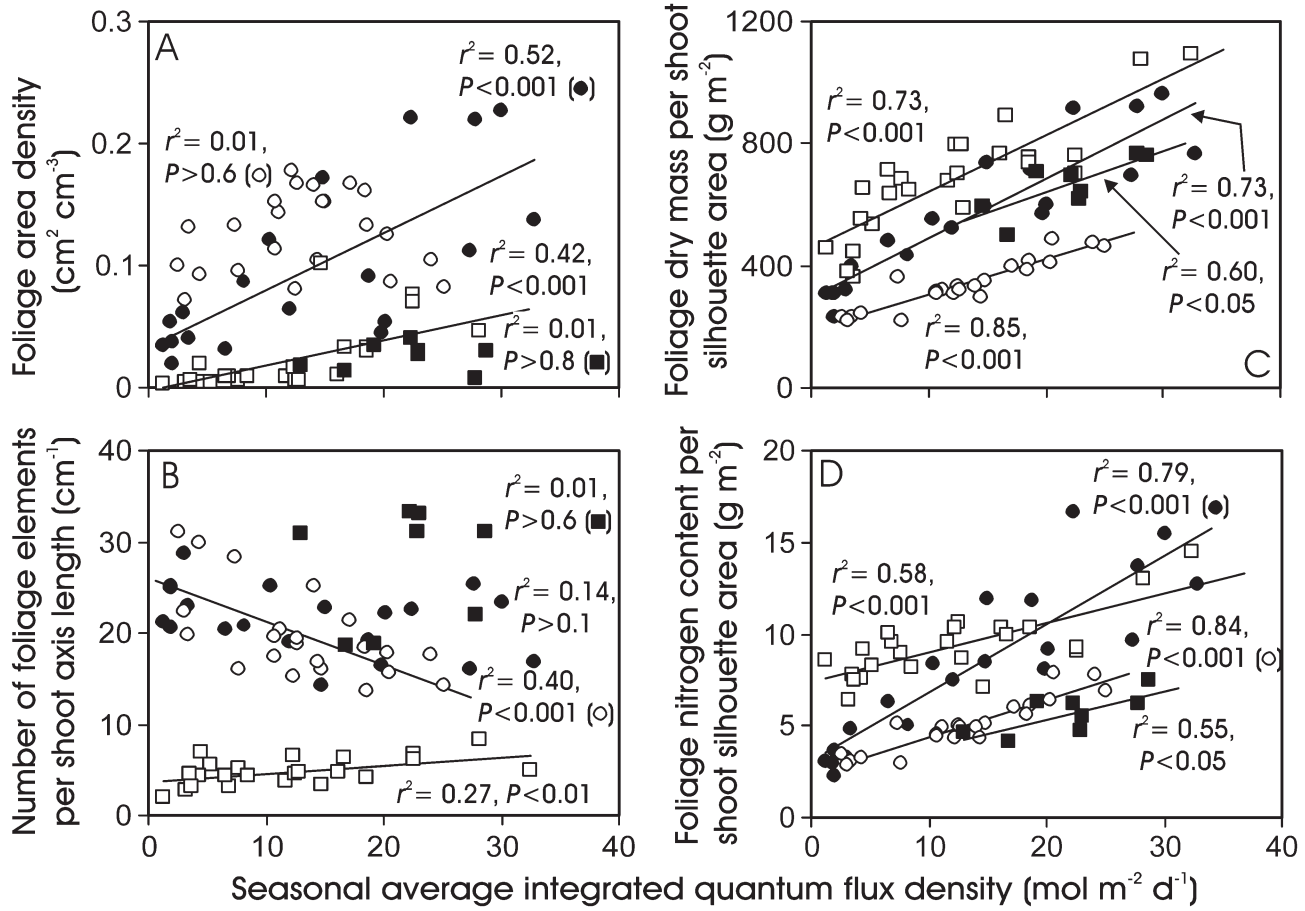


**Fig. 4** Foliage area density (*A*; eq. [1]), number of needles per shoot axis length (*B*), foliage dry mass per unit shoot silhouette area (*C*; $M_S$; projection $0°, 0°$), and foliage nitrogen content per unit shoot silhouette area (*D*; $N_S$) in relation to quantum flux density in *Casuarina glauca*, *Pinus palustris*, *P. patula*, and *P. radiata*. Foliage area density is given as the density of half of the total area. $N_S$ is equal to $M_S$ times foliage nitrogen content per dry mass ($N_M$). Data fitting and symbols as in fig. 2.

Five needles for pines and five cladodes for *Casuarina* were randomly taken from the shoot for foliage element area determinations. For *Pinus* species with needle shape approximated as a sector of a circle, the needle area was calculated from measurements of thickness and width by digital precision calipers (Mitutoyo CD-15DC, Mitutoyo, Andover, UK) and measurements of needle length according to equations provided by Niinemets et al. (2002*b*). In *Casuarina*, that has a cylindrical cladode cross-section (Niinemets et al. 2005*a*), cladode area was determined from measurements of cladode diameter and length. The ratio of foliage element length to cross-section area was calculated as a relative estimate of bending resistance of foliage.

Sample foliage was dried at 70°C for at least 48 h, and dry mass was determined. The rest of the needles were also weighed after drying, and the total foliage area was determined from the values of dry mass per unit area ($M_A$) of sample foliage and the total dry mass of foliage on the shoot. Foliage nitrogen ($N_M$) content was determined with a LECO CNS-2000 analyzer (Laboratory Equipment, St. Joseph, MI).

The shoot silhouette area measurements include the visible area of the shoot axis. Shoot axis area, $A_A(0°, 0°)$, was calculated from the shoot axis length and measurements of shoot axis basal and apical diameters in perpendicular directions. Shoot axis area was included in the shoot radiative model. After the morphological measurements, the woody biomass was dried at 70°C for at least 48 h, and the dry mass was determined. Details of *P. sylvestris* needle and shoot measurements are provided by Niinemets et al. (2002*a*).

### *Shoot Light-Interception Model*

To separate between the effects of various shoot architectural traits that determine the shoot radiative transfer, we apply the shoot model of Cescatti and Zorer (2003) and Niinemets et al. (2002*a*). In this model, the shoot is approximated as a cylinder with an elliptical cross-section that is filled with a turbid medium. The probability of photon interception in the shoot volume, $F(\phi, \varphi)$, is further simulated using the theory of light penetration in nonrandom media:

$$F(\phi, \varphi) = 1 - \exp[-G(c, \gamma)\lambda_0 \rho L_B(\phi, \varphi)], \quad (2)$$

where the $G(c, \gamma)$ function is the extinction coefficient (Ross 1981), $\lambda_0$ is the Markov coefficient of spatial clumping (Nilson 1971), $\rho$ is the foliage area density in the shoot volume (eq. [1]), and $L_B(\phi, \varphi)$ is the beam path length in the shoot volume for specific shoot rotation ($\phi$) and inclination ($\varphi$) angles. The Markov coefficient is a measure of within-shoot spatial aggregation and ranges from 1 (random distribution) to 0 (completely aggregated distribution). For a common total foliage area, shoots with clumped foliage dispersion intercept less light than the shoots with random dispersion. The angle between the normal to the shoot plane $(0°, 0°)$ and the direction of illumination is $\gamma$, and this varies with both the shoot inclination and rotation angles:

$$\gamma = \arccos(\cos\phi \cos\varphi). \quad (3)$$

We use the ellipsoidal foliage surface angle distribution for the $G(c, \gamma)$ function (Campbell 1986):

$$G(c, \gamma) = \frac{\sqrt{c^2 \cos^2\gamma + \sin^2\gamma}}{Bc}. \quad (4)$$

The parameter $c$ is the ratio of the ellipsoid horizontal to vertical semiaxes, and $B$ is given as

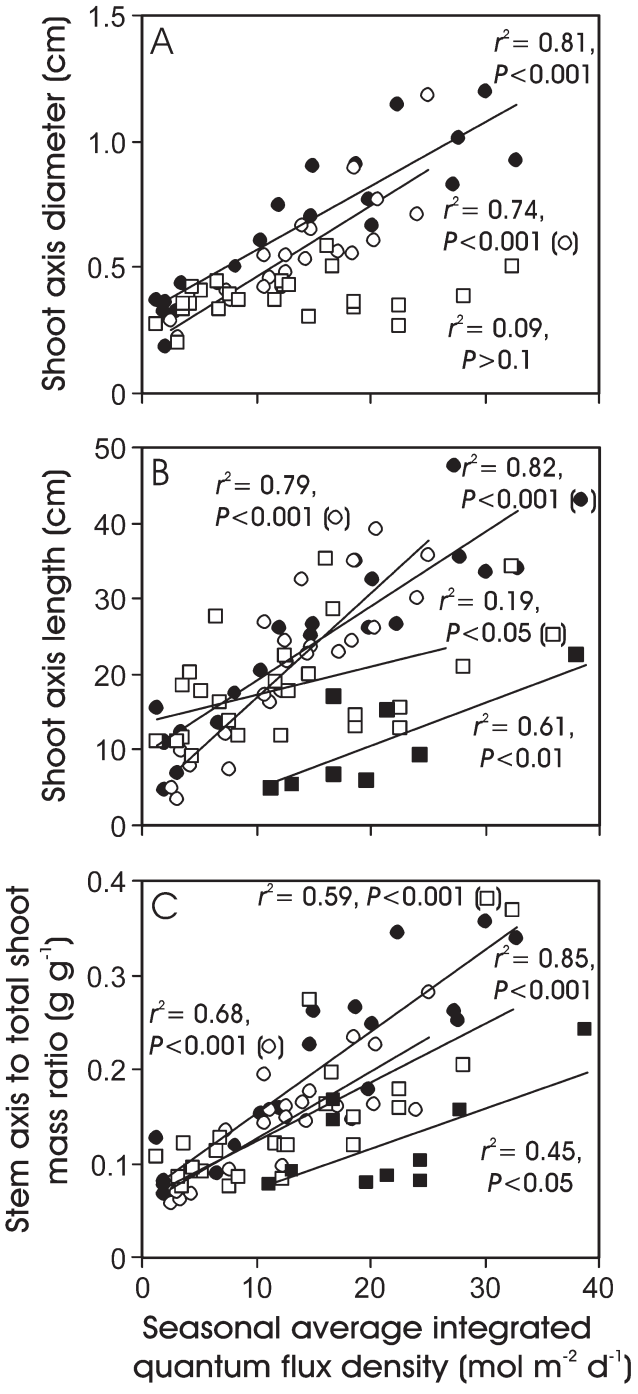


**Fig. 5** Light-dependent changes in shoot axis diameter (*A*), length (*B*) , and stem axis to total shoot mass ratio (C) in *Casuarina glauca*, *Pinus palustris*, *P. patula*, and *P. radiata*. Data fitting and symbols as in fig. 2.

$$B = \begin{cases} 1 + \dfrac{\ln\left[(1+\sqrt{1-c^{-2}})/(1-\sqrt{1-c^{-2}})\right]}{2c^2\sqrt{1-c^{-2}}}, & \text{if } c > 1 \\ 1 + \dfrac{\sin^{-1}\sqrt{1-c^2}}{c\sqrt{1-c^2}}, & \text{if } c < 1 \end{cases}. \quad (5)$$

Foliage surface area distributions with $c > 1$ are horizontal, while the distributions with $c < 1$ are vertical, and $c = 1$ for a spherical distribution. Equation (4) assumes that the distribution of leaf azimuth angles is uniform (Campbell 1986). Further details of the shoot radiative transfer model are provided by Niinemets et al. (2002*a*) and Cescatti and Zorer (2003).

### *Model Parameterization*

The predicted shoot silhouette area for specific view directions $A'_S(\phi, \varphi)$ is equal to the probability of photon interception $F(\phi, \varphi)$ times the projected area of the shoot cylinder with elliptical cross-section (elliptical cylinder) $A_{SC}(\phi, \varphi)$:

$$A'_S(\phi, \varphi) = A_A(\phi, \varphi) + F(\phi, \varphi)[A_{SC}(\phi, \varphi) - A_A(\phi, \varphi)], \quad (6)$$

where $A_A(\phi, \varphi)$ is the projected area of shoot axis that is included to account for the shading by the shoot axis. The unknowns, the angular distribution of leaf normals ($c$) and the coefficient of spatial aggregation ($\lambda_0$), were determined by iteratively minimizing the square error ($E$) between the observed, $A_S(\phi, \varphi)$, and simulated, $A'_S(\phi, \varphi)$, shoot silhouette areas:

$$\min E = \sum_{\phi} \sum_{\varphi} [A'_S(\phi, \varphi) - A_S(\phi, \varphi)]^2. \quad (7)$$

Overall, the five projections measured generally predict the shoot silhouette areas with a high degree of explained variance ($r^2 = 0.8 - 0.9$) (Bernier et al. 2001; Cescatti and Zorer 2003; Niinemets et al. 2004, 2005*b*) and thus result in reliable values of both parameters $c$ and $\lambda_0$. Given that the parameter $c$ correlates strongly with the ratio of shoot projections $A_S(0°, 0°)/A_S(90°, 0°)$, while the ratio of $A_S(0°, 0°)$ to total needle area correlates strongly with the parameter $\lambda_0$ (Cescatti and Zorer 2003), the two shoot silhouette projections $(0°, 0°)$ and $(90°, 0°)$ measured in *P. palustris*, *P. sylvestris*, and *P. taeda* also yield realistic values of the model parameters (Niinemets et al. 2002*a*; Cescatti and Zorer 2003). However, in *P. patula*, with strongly bending needles, we lacked the shoot projection $(90°, 0°)$. While the clumping index, $\lambda_0$, could still be reliably derived from the three measured projections, missing data for the $(90°, 0°)$ projection implies that the derived values of needle angular distribution (parameter $c$) in this species are not directly comparable with $c$ estimates in other species. Nevertheless, the values of $c$ were consistently derived for all shoots of this species and still provide a means to assess the light-dependent trends on needle angular distribution within the canopy.

### *Characterization of Light-Interception Efficiency*

The parameterized model was employed to predict the silhouette area at different inclination and rotation angles by equation (6), with a resolution of 5° for both $\varphi$ and $\phi$ to obtain the spherically averaged shoot silhouette area, $\overline{A'_S}$:

$$\overline{A'_S} = \frac{1}{2\pi} \int_{-\pi/2}^{\pi/2} \int_{-\pi/2}^{\pi/2} A'_S(\phi, \varphi) \cos\varphi \, d\varphi \, d\phi. \quad (8)$$

This equation was integrated by fitting a quadratic spline function through the predicted values of $A'_S(\phi, \varphi)$ as in Cescatti

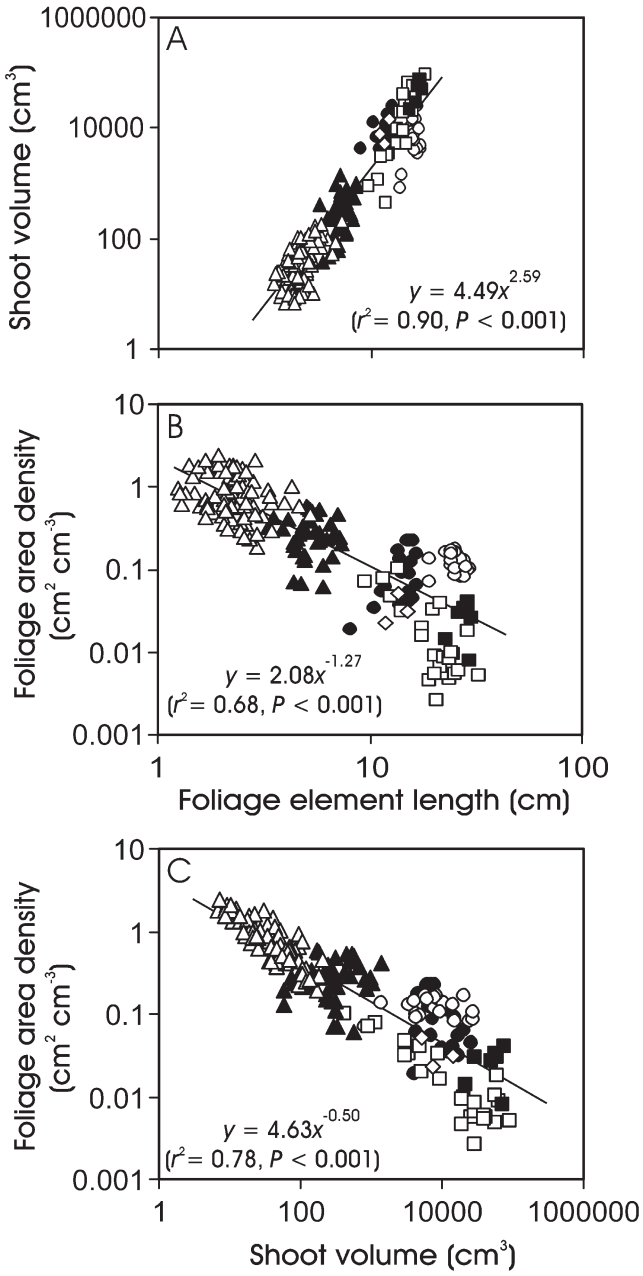


**Fig. 6** Correlations of shoot volume (*A*) and foliage area density (*B*) with foliage element length and correlation between foliage area density and shoot volume (*C*) in *Casuarina glauca*, *Pinus palustris*, *P. patula*, and *P. radiata* (symbols as in fig. 2), and in *P. sylvestris* from infertile (open triangle) and fertile site (filled triangle) and in *P. taeda* (open diamond). Linear regressions lines to all data pooled are also provided.

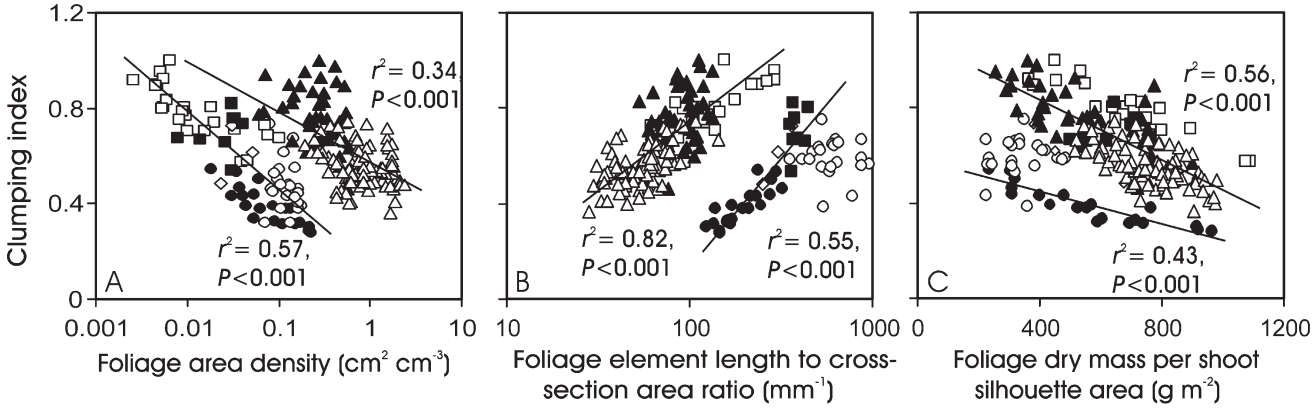


**Fig. 7** Clumping index (eq. [2]) in relation to foliage area density (*A*), foliage length to cross-section area ratio (*B*), and foliage dry mass per shoot silhouette area (*C*) in *Casuarina glauca*, *Pinus palustris*, *P. patula*, *P. radiata*, *P. sylvestris* from infertile and fertile sites, and *P. taeda* (symbols as in fig. 6). Foliage length to cross-section area ratio was used to account for the different stiffness and bending of foliage elements with common length. Data were fitted by linear regressions. In *A*, data of *P. sylvestris* from infertile and fertile sites were fitted separately. In *B*, separate regression lines were fitted to foliage with circular (*C. glauca*) and hemicircular cross-section geometry (*P. sylvestris*) and to *P. palustris*, *P. radiata*, and *P. taeda*, which have needles with a sectorial shape on cross-section. In *C*, a separate regression line is provided for *P. patula* and *P. radiata*.

and Zorer (2003). The estimate of $\overline{A'_S}$ was used to calculate the spherically averaged silhouette to total leaf area ratio, $\overline{S_S}$, which is a measure of the relative efficiency of diffuse radiation interception (Stenberg et al. 2001; Cescatti and Zorer 2003). For uniformly overcast sky, the mean diffuse quantum flux density on foliage area is given by $2\overline{S_S}$ times the incident quantum flux density.

One-sided sunlit area ($\delta_S$), the ratio of shoot silhouette area to half of the total needle area projected onto an orthogonal plane, was calculated for a population of shoots with uniform azimuth distribution to estimate the efficiency of direct radiation capture (Niinemets et al. 2002*a*; Cescatti and Zorer 2003):

$$\delta_S(\phi,\varphi) = \frac{2A_S(\phi,\varphi)}{A_L G(c,\gamma)} = \frac{2S_S(\phi,\varphi)}{G(c,\gamma)}. \quad (9)$$

Equation (9) provides the fraction of exposed needle area for any combination of shoot inclination and rotation angles.

### Data Analyses

Linear regression analyses were used to test for the significant effects of average integrated irradiance ($Q_{int}$) on shoot structural characteristics. The statistical differences among the regressions were separated by analyses of covariance (ANCOVA). A separate-slope model that includes an interaction term Species × $Q_{int}$ was used first. When the interaction term was nonsignificant, a common-slope ANCOVA was employed to test for the significant intercept differences (Sokal and Rohlf 1995).

The light-acclimation characteristics of *P. sylvestris* shoots are reported in detail by Niinemets et al. (2002*a*). The data for this species and for *P. taeda*, for which we had a limited sample size, were used with the data for other species to explore the general correlations among foliage size and light-harvesting efficiency characteristics. To linearize the relationships, it was necessary to log-transform the pooled data in several cases. All statistical effects were considered significant at $P < 0.05$.

## Results

### Acclimation of Shoot Radiative Characteristics

The shoot silhouette to total foliage area ratio for the rotation and inclination angle pair (0°, 0°), $S_S(0°, 0°)$, that generally provides the maximum amount of shade produced by a unit foliage area was negatively associated with seasonal average integrated quantum flux density ($Q_{int}$) in all species except *Pinus patula* (fig. 2*A*). The light relationships of average silhouette ($\overline{S_S}$; eq. [6]) to total foliage area ratio that characterizes the efficiency of diffuse light harvesting were similar to $S_S(0°, 0°)$ ($r^2 = 0.66$, $P < 0.001$ for *Casuarina glauca*; $r^2 = 0.62$, $P < 0.02$ for *P. palustris*; $r^2 = 0.00$, $P > 0.9$ for *P. patula*; and $r^2 = 0.65$, $P < 0.001$ for *P. radiata*). The sunlit foliage area fraction ($\delta_S$; eq. [9]) was negatively related to irradiance in *P. palustris* ($r^2 = 0.63$, $P < 0.02$) and *P. radiata* ($r^2 = 0.62$, $P < 0.001$), but $\delta_S$ was independent of irradiance in *P. patula* ($r^2 = 0.02$, $P > 0.5$) and *C. glauca* ($r^2 = 0.01$, $P > 0.7$).

The parameter *c* of the ellipsoidal needle area distribution (eqq. [4], [5]) was positively related to irradiance in *P. patula* and *C. glauca*, but the correlation was weak (fig. 2*B*). These correlations were positive, demonstrating that foliage angles became more horizontal in higher light (fig. 2*B*). The clumping index ($\lambda_0$) was negatively correlated with light in all species except for *P. patula* (fig. 2*C*), indicating the general increase of foliage aggregation with increasing irradiance.

Shoot inclination angles with respect to horizontal ($\varphi$) in shoot natural location in the canopy were measured in three species. In all these species, $\varphi$ increased with increasing light in three studied species (fig. 3), but in *P. patula* and *C. glauca* the angles were more negative at low light; i.e., the shoots were hanging downward.

As the covariation analyses demonstrated, the slopes of $S_S(0°, 0°)$, $\overline{S_S}$, and $\lambda_0$ versus $Q_{int}$ relationships (fig. 2*A*, 2*C*) were affected by species ($P < 0.001$). This resulted from significantly lower plasticity in *P. patula*, which has strongly bending needles. At a common irradiance, *C. glauca* had the highest $S_S(0°, 0°)$ (fig. 2*A*) and the highest sunlit cladode area fraction (average ± SE = 0.854 ± 0.014), and *P. palustris* and *C. glauca* had the highest $\overline{S_S}$ (0.144 ± 0.006 for *P. palustris* and 0.2149 ± 0.0036 for *C. glauca*) and clumping index (fig. 2*C*). In contrast, *P. radiata*, with the shortest foliage elements of the four species (table 1) had the lowest $S_S(0°, 0°)$ (fig. 2*A*), $\overline{S_S}$ (average ± SE = 0.090 ± 0.005), $\lambda_0$ (fig. 2*C*), and sunlit needle area fraction (average ± SE = 0.355 ± 0.018).

### *Light-Dependent Accumulation of Shoot Biomass and Nitrogen per Unit Area*

Foliage area density (eq. [1]) increased with increasing irradiance in *P. radiata* and *C. glauca* and was not related to light in *P. palustris* and *P. patula* (fig. 4*A*). The number of foliage elements per unit shoot axis length increased with increasing $Q_{int}$ in *C. glauca*, but it decreased in *P. patula* and was independent of $Q_{int}$ in *P. palustris* and *P. radiata* (fig. 4*B*). At a common irradiance, the foliage area density was less in *P. palustris* and *C. glauca* than in the other two species ($P < 0.001$), while the foliage element number per unit shoot axis length was the lowest in *C. glauca* (fig. 4*B*, $P < 0.001$).

Foliage dry mass per unit shoot silhouette area ($M_S$), which is given as the foliage element mass per surface area ($M_A$) divided by $S_S(0°, 0°)$, was positively associated with $Q_{int}$ in all species (fig. 4*C*). The increase in $M_S$ with light provided the primary explanation for the scaling of foliage nitrogen contents per silhouette area ($N_S = N_M M_S$, where $N_M$ is the foliage nitrogen content per unit dry mass) with irradiance (fig. 4*D*).

The slopes of $M_S$ versus $Q_{int}$ relations were not different ($P > 0.06$ according to a separate-slope ANCOVA analyses), while at a common $Q_{int}$, $M_S$ was the largest in *C. glauca* and smallest in *P. patula*. This was mainly because of species differences in $M_A$ (average ± SE = 154 ± 5 g $m^{-2}$ in *C. glauca* vs. 47.4 ± 2.5 g $m^{-2}$ in *P. patula*, 97.1 ± 1.6 g $m^{-2}$ in *P. palustris*, and 64.6 ± 3.4 g $m^{-2}$ in *P. radiata*). Species differences in $N_S$ to $Q_{int}$ relations were associated with species variation in average $N_M$ and differences in $N_M$ versus $Q_{int}$ relations.

### *Support Costs of Different Architectural Designs*

Shoot axis diameter (fig. 5*A*) and shoot length (fig. 5*B*) increased with increasing irradiance, except for the axis diameter in *C. glauca* (fig. 5*A*). The fractional shoot biomass investment in shoot axis increased with increasing light (fig. 5*C*). Thus, these results collectively indicate that the support investments increased with increasing shoot size and light availability. At high irradiance, the shoot axis diameter was lower in *C. glauca* than in the other species, while the shoot length and fractional biomass investment in shoot axis were lower in *P. palustris* than in the other species ($P < 0.002$ for intercept differences).

### *Do Shoots with Varying Size Harvest Light Differently?*

For all data pooled, shoot length and foliage element length were positively correlated ($r^2 = 0.62$, $P < 0.001$ for $y = ax^b$ allometric relationship) with a scaling exponent $b = 0.799$. Given this allometric scaling, and given that increases in foliage length affect both shoot width and height (eq. [1]), all else being equal, if foliage length doubles, shoot cross-section should quadruple and shoot volume increase approximately sixfold. In a close agreement with this prediction, the allometric relationship between shoot volume and foliage element length had a scaling exponent of 2.59, i.e., 6.02-fold increase in shoot volume for a doubling of foliage length for all data pooled (fig. 6*A*). As foliage length scales linearly with foliage area (scaling exponent $b = 1$), the predicted scaling exponent of the relationship between foliage length and needle area density ($\rho$; eq. [1]) is $b = 1 - 2.59 = -1.59$; i.e., all else being equal, doubling of foliage length should result in an approximately three-fold reduction in $\rho$. We found a scaling exponent of −1.27 for this relationship (fig. 6*B*), implying ca. 2.5-fold reduction of $\rho$ for a doubling of foliage length. Although equation (1) predicts an inversely proportional relationship between shoot volume and $\rho$, the scaling exponent for this relationship was −0.5 (fig. 6*C*), and thus, doubling of shoot volume resulted in ca. 1.5-fold reduction in foliage area density.

These differences from the theoretical predictions resulted partly from the circumstance that, at a common foliage length, strongly bending needles of *P. patula* had a greater $\rho$ than the other species ($P < 0.001$ for common-slope comparisons with *P. palustris*, *P. radiata*, *P. taeda*, and *C. glauca*; fig. 6*B*). As all needles are bent downward in shoots of *P. patula*, doubling of foliage element length results in doubling of shoot cylinder cross-section rather than in quadrupling, as in the other species (fig. 1).

Foliage clumping increased (lower value of $\lambda_0$) with increasing $\rho$ (fig. 7*A*), but the clumping decreased with increasing foliage element length and foliage element length to cross-section ratio (fig. 7*B*), demonstrating an overall greater light-interception efficiency of shoots with more sparse foliage. Analogous correlations were found between $\rho$, foliage length, and average shoot silhouette to total area ratio ($\overline{S_S}$) and sunlit foliage area fraction ($\delta_S$, eq. [9]; data not shown). The correlations were weaker with foliage length than with foliage length to cross-section ratio, which partly accounts for the variations in bending of foliage elements of the same length but different cross-section areas.

At a common foliage area density, the shoots were less clumped in *P. sylvestris* from both fertile and infertile sites ($P < 0.001$; fig. 7*A*). At a common foliage length to cross-section ratio, the species with three-needled fascicles had a greater degree of foliage aggregation than the two-needled species *P. sylvestris* and *C. glauca*, which have the cladodes directly attached to the stem ($P < 0.001$; fig. 7*B*).

The degree of foliage clumping and dry mass per silhouette area ($M_S$) were positively associated (lower $\lambda_0$), indicating greater packing of photosynthetic biomass in more strongly aggregated shoots (fig. 7*C*). At a common $M_S$, the foliage of *P. radiata* and *P. patula* was more strongly aggregated than that in the other species ($P < 0.001$; fig. 7*C*).

## Discussion

### *Acclimation of Shoot Light-Harvesting Efficiency to Long-Term Irradiance*

The shoot light model (eqq. [2]–[5]) gives comparable shoot radiative transfer characteristics for the shoots of different size and architecture and provides a tool for rigorous intra- and interspecific comparisons. The model separates the changes in light-harvesting efficiency resulting from spatial aggregation, angular distribution of foliage elements, and the density of foliage area. In *Pinus palustris*, *P. radiata*, and *Casuarina glauca*, increases in light availability resulted in lower fraction of exposed to total foliage area (fig. 2*A*), as is commonly observed in conifers (Sprugel et al. 1996; Stenberg et al. 1998, 2001; Niinemets et al. 2002*a*; Cescatti and Zorer 2003).

In our study, decreases in light-harvesting efficiency in high light were associated mainly with a greater degree of foliage aggregation in high light (cf. fig. 2*B* and fig. 2*C*), as has been previously reported for *P. sylvestris* (Niinemets et al. 2002*a*). In contrast, in shade-tolerant conifers such as *Abies* (Cescatti and Zorer 2003) and *Picea* (Niinemets and Kull 1995), acclimation to low irradiance involved not only reduced clumping but also more horizontal foliage inclination-angle distributions (greater values of *c*). Such modifications in foliage inclination-angle distributions result in more efficient light capture in forest understories, where most of the direct light penetrates under low zenith angles. Although in our study the absolute values of the ellipsoidal needle area distribution (*c*; eqq. [4], [5]) are not directly comparable between species with stiff and bending needles (see "Methods"), within-canopy variation in the estimates of *c* suggested that the distribution of foliage inclination angles became slightly more vertical rather than horizontal with decreasing irradiance in the species with bending needles (fig. 2*B*), indicating that modification of foliage surface inclination-angle distribution did not play a role in light acclimation in these shade-intolerant conifers. In fact, more horizontal foliage inclinations in higher light in *P. patula* probably reflect greater stiffness of needles with larger cross-sectional areas in high irradiance. Nonplastic foliage angular distributions also have been found in the shade-intolerant conifer *P. sylvestris* (Niinemets et al. 2002*a*). Overall, these data demonstrate that the possibility to control leaf angle is dependent on foliage element length. Only species with short needles (*Abies*, *Picea*, *Pseudotsuga*) are able to increase *c* in low light.

### *Species Variation in Shoot Light-Harvesting Efficiency*

Previous studies have demonstrated convergent light-harvesting efficiency of broad-leaved species with varying architectural attributes (Valladares et al. 2000, 2002; Niinemets et al. 2004). We observed significant canopy and species differences in shoot light-interception efficiency that resulted from different combinations of leaf area density, angular distribution of leaf surface, and spatial aggregation of foliage elements within the shoot volume (fig. 2). *Casuarina glauca*, the species with the least densely foliated shoots and one of the species with the longest foliage elements (fig. 1, table 1), had the largest values of shoot silhouette to total area ratio (fig. 2*A*) and the lowest degree of foliage aggregation (fig. 2*C*). In contrast, *P. radiata* had large foliage area density (fig. 4*A*) and medium needle lengths (table 1), which resulted in the lowest silhouette to total area ratios (fig. 2*A*) and the greatest foliage aggregation and self-shading (fig. 2*C*).

*Pinus patula*, with weeping needles, was a nonplastic species in our study (fig. 2). Such a nonplastic response to irradiance was associated with the inflexibility in needle spacing in the shoot volume because of strong needle bending. This strong needle bending resulted in similar estimates of spatial aggregation in both low and high light (fig. 2*C*). Nevertheless, the clumping in *P. patula* was still less than in *P. radiata* (fig. 2*C*), possibly because of greater needle length and downward-elongated shoot form in *P. patula* that resulted in lower shading by the stem axis and neighboring needles.

Of course, because of strong bending, the shoot light-interception characteristics of *P. patula* shoots were derived using a modified procedure that included only the shoot projections with horizontal stem axis and the projection with the stem axis in shoot natural position. Although this may affect the exact values of the efficiency characteristics derived from the model, directly measured characteristics such as the amount of shadow produced by unit foliage area (fig. 2*A*) and foliage area density (fig. 4*A*) were also independent of irradiance. Thus, it is unlikely that the analysis modifications affected our conclusion of the nonplastic light-harvesting efficiency in *P. patula*.

### *Accumulation of Foliage Biomass in Light Gradients*

Foliage biomass ($M_S$; fig. 4*C*) and nitrogen ($N_S$; fig. 4*D*) accumulation per unit shoot silhouette area at higher irradiance, as observed in all species of our study, is a general feature in conifers (Niinemets and Kull 1995; Sprugel et al. 1996; Niinemets et al. 2002*a*; Cescatti and Zorer 2003). In several conifers, greater needle number per unit shoot axis length at higher irradiance (Niinemets and Kull 1995; Niinemets et al. 2002*a*; Leal and Thomas 2003) partly explains the increase in $M_S$ and $N_S$ with light. However, in our study, larger cladode number per unit stem length was only observed in *C. glauca* (fig. 4*B*). In fact, light-dependent changes in $M_S$ and $N_S$ were primarily associated with changes in shoot (silhouette to total area ratio, $S_S$) and foliage morphology (foliage dry mass per unit area, $M_A$; $M_S = M_A/S_S$).

Although greater foliar biomass investment in high light is compatible with a lower light-harvesting efficiency, this response results in greater photosynthetic biomass in high-light environments where the photosynthetic returns are the largest. Theoretical studies have suggested that there is a general trade-off between nitrogen and light-use efficiencies in plant canopies (Hirose and Bazzaz 1998), and our results further underscore the relevance of this compromise between light harvesting and shoot photosynthetic potentials.

Species differences in foliage mass (fig. 4*C*) and nitrogen content (fig. 4*D*) per silhouette area versus irradiance relationships demonstrate that the overall significance of this trade-off depends on the acclimation in shoot architecture (fig. 2), foliage morphology (foliage dry mass per total area), and foliage nitrogen contents per dry mass. Apart from photosynthetic gains, greater foliage aggregation in high light has also been interpreted as a light-avoidance strategy in environments where high irradiance interacts with other environmental constraints, resulting in severe photoinhibition of

photosynthetic apparatus (Valladares and Pugnaire 1999; Pearcy et al. 2005). Given that soil drought is common in the habitats of shade-intolerant conifers, enhanced foliage clumping in high light can also play a significant role in minimizing the photoinhibition effects on daily photosynthetic production in the species studied here.

### *Support Investments and Light Harvesting*

The shoots became longer and had thicker axes in higher light in most species (fig. 5*A*, 5*B*). The fractional investment in shoot axis biomass scaled positively in light in all species (fig. 5*C*), as has been previously observed in *Abies balsamea* (Niinemets and Lukjanova 2003). Thus, the costs for foliage support increase disproportionately with light in the canopy. This disproportionate increase in fractional support investments is associated with longer and heavier shoots as well as greater water requirements of foliage exposed to higher irradiance.

Except for lower fractional support investments in *P. palustris*, the species differences were small at a common irradiance (fig. 5*C*). However, for stiff needles, the shoots with longer foliage elements have effectively longer lever arms and have greater support requirements. For long, bending needles, the mass is also effectively distributed farther away from the axis of bending, again implying augmented support requirements to counteract larger static and dynamic loads. In fact, the shoots of *C. glauca* and *P. patula* had negative inclination angles in low light (fig. 3). The shoots hanging downward have lower support requirements but also lower light-harvesting efficiencies than the horizontal shoots. This reasoning suggests that in *C. glauca* and *P. patula*, limited support investments may have reduced the shoot light-harvesting efficiency in low light.

### *Light-Harvesting Efficiency in Relation to Foliage and Shoot Size*

The shoots of the studied conifers mainly differed in the number of foliage elements per stem axis length, in the size of shoots and foliage elements, and in the degree of foliage bending (*P. patula* vs. the other species; fig. 1). The data collectively demonstrate that longer foliage elements are associated with less dense shoot volumes (fig. 6) and lower degree of clumping of foliage elements (fig. 7*A*, 7*B*). Simulation studies in broad-leaved species demonstrate that increasing petiole length and leaf length to width ratio is a major way to enhance light interception by reducing the self-shading within the shoot (Takenaka 1994; Pearcy and Yang 1998). Thus, we suggest that the increase in conifer foliage length represents a convergent adaptation to reduce within-shoot shading.

Three-needled species were standing out in the relationships between spatial aggregation and foliage length to cross-section area ratio (fig. 7*B*). As the single foliage elements and two-needled fascicles can be more flexibly spaced on the shoot axis, the greater clumping in three-needled species can be explained partly by inherently larger aggregation from their fascicle structure. In addition, mechanical theory predicts that at a common cross-sectional area, the needles with circular and hemicircular cross-sections bend less than the needles with a cross-sectional geometry of a circle sector (Gere and Timoshenko 1997). Thus, a greater gap fraction in the shoot volume in the three-needled species also may be associated with their relatively greater degree of bending because of sectorial needle cross-section geometry. In particular, in *P. patula*, with very strongly bending needles, the relationship between the spatial aggregation and needle length to cross-section ratio was lost because the foliage clumping actually increases for strong bendings, as the needles are more closely adhered together.

Overall, the species with long foliage elements form open canopies with minimum below-canopy irradiances of 0.1–0.5 (Brockway and Outcalt 1998; Battaglia 2000; Shelton and Cain 2000; Lemeniha et al. 2004; Yirdaw and Luukkanen 2004). As our study demonstrates, the light-harvesting efficiency of species with long foliage elements is not inherently low. However, maintenance of high light-harvesting efficiency is bound to sparsely foliated shoots that do not cast deep shade. In addition, as excessive foliage bending results in a greater degree of foliage aggregation, larger irradiances may be required for species with long foliage for construction of bending-resistant foliage with large cross-sectional areas.

Enhanced clumping in species with shorter foliage results in greater foliage dry mass per unit shoot silhouette area (fig. 7*C*), further underscoring the general trade-off between light-use efficiency and shoot photosynthetic potentials that contributes toward the maximization of whole-tree photosynthetic activity in conifer stands. Overall, these data demonstrate that in shade-intolerant conifers, light primarily affects the degree of foliage clumping, and that the species differences in foliage aggregation are associated with the density of foliage elements on the shoots, length of foliage elements, and the degree of foliage bending.

## Acknowledgments

We thank David S. Ellsworth for the help in the field. The experimental part of the study was mainly conducted when Ü. Niinemets was a visiting Erskine fellow of the University of Canterbury, Christchurch, New Zealand. Additional financial support was provided by the Estonian Science Foundation (grant 5702), the Estonian Ministry of Education and Science (grant 0182468As03), the German Academic Exchange Service, the National Research Council, National Academy of Sciences, USA (Twinning Program, COBASE), and the Province of Trento, Italy (grants DL1060 and DL3402).

## Literature Cited

Battaglia MA 2000 The influence of overstory structure on understory light availability in a longleaf pine (*Pinus palustris* Mill.) forest. MS thesis. Virginia Polytechnic Institute and State University, Blacksburg.

Berg RH 1994 A calcium oxalate-secreting tissue in branchlets of the Casuarinaceae. Protoplasma 183:29–36.

Bernier PY, F Raulier, P Stenberg, C-H Ung 2001 Importance of needle age and shoot structure on canopy net photosynthesis of

balsam fir (*Abies balsamea*): a spatially inexplicit modeling analysis. Tree Physiol 21:815–830.

Boyer WD 1990 *Pinus palustris* Mill. longleaf pine. Pages 405–412 *in* RM Burns, BH Honkala, eds. Silvics of North America. USDA Forest Service Agriculture Handbook 654. Washington, DC.

Brockway DG, KW Outcalt 1998 Gap-phase regeneration in longleaf pine wiregrass ecosystems. For Ecol Manag 106:125–139.

Burns RM, BH Honkala, eds 1990 Silvics of North America. USDA Forest Service Agriculture Handbook 654. Washington, DC.

Campbell GS 1986 Extinction coefficients for radiation in plant canopies calculated using an ellipsoidal inclination angle distribution. Agric For Meteorol 36:317–321.

Cescatti A, Ü Niinemets 2004 Sunlight capture: leaf to landscape. Pages 42–85 *in* WK Smith, TC Vogelmann, C Chritchley, eds. Photosynthetic adaptation: chloroplast to landscape. Ecological studies, vol 178. Springer, Berlin.

Cescatti A, R Zorer 2003 Structural acclimation and radiation regime of silver fir (*Abies alba* Mill.) shoots along a light gradient. Plant Cell Environ 26:429–442.

Chen JM, TA Black 1992 Defining leaf area index for non-flat leaves. Plant Cell Environ 15:421–429.

Dougherty PM, LH Allen, LW Kress, R Murthy, CA Maier, TJ Albaugh, DA Sampson 1998 An investigation of the impacts of elevated carbon dioxide, irrigation, and fertilization on the physiology and growth of loblolly pine. Pages 149–168 *in* RA Mickler, S Fox, eds. The productivity and sustainability of southern forest ecosystems in a changing environment. Springer, Berlin.

Dutta RK, M Agrawal 2001 Litterfall, litter decomposition and nutrient release in five exotic plant species planted on coal mine spoils. Pedobiologia 45:298–312.

Ellsworth DS 2000 Seasonal $CO_2$ assimilation and stomatal limitations in a *Pinus taeda* canopy. Tree Physiol 20:435–445.

Gere JM, SP Timoshenko 1997 Mechanics of materials. PWS, Boston.

Hale SE, C Edwards 2002 Comparison of film and digital hemispherical photography across a wide range of canopy densities. Agric For Meteorol 112:51–56.

Harcombe PA, JS Glitzenstein, RG Knox, SL Orzell, EL Bridges 1993 Vegetation of the longleaf pine region of the West Gulf coastal plain. Pages 83–104 *in* SM Hermann, ed. Proceedings of the Tall Timbers Fire Ecology Conference. Tall Timbers Research Station, Tallahassee, FL.

Hirose T, FA Bazzaz 1998 Trade-off between light- and nitrogen-use efficiency in canopy photosynthesis. Ann Bot 82:195–202.

Immel DL 2002 Monterey pine (*Pinus radiata* D. Don). USDA Natural Resources Conservation Service Plant Guide. http://plants.usda.gov.

Langeland KA, K Craddock Burks 1998 Identification and biology of non-native plants in Florida's natural areas. University of Florida, Gainesville. 165 p.

Leal DB, SC Thomas 2003 Vertical gradients and tree-to-tree variation in shoot morphology and foliar nitrogen in an old-growth *Pinus strobus* stand. Can J For Res 33:1304–1314.

Lemeniha M, T Gidyelewa, D Teketay 2004 Effects of canopy cover and understory environment of tree plantations on richness, density and size of colonizing woody species in southern Ethiopia. For Ecol Manag 194:1–10.

Linder S 1987 Responses to water and nutrients in coniferous ecosystems. Pages 180–202 *in* ED Schulze, H Zwölfer, F Golley, OL Lange, JS Olson, H Remmert, eds. Potentials and limitations of ecosystem analysis. Ecological studies, vol 61. Springer, Berlin.

Murthy R, PM Dougherty 1997 Effect of carbon dioxide, fertilization and irrigation on loblolly pine branch morphology. Trees 11: 485–493.

Niinemets Ü, A Cescatti, R Christian 2004 Constraints on light interception efficiency due to shoot architecture in broad-leaved *Nothofagus* species. Tree Physiol 24:617–630.

Niinemets Ü, A Cescatti, A Lukjanova, M Tobias, L Truus 2002*a* Modification of light-acclimation of *Pinus sylvestris* shoot architecture by site fertility. Agric For Meteorol 111:121–140.

Niinemets Ü, DS Ellsworth, A Lukjanova, M Tobias 2001 Site fertility and the morphological and photosynthetic acclimation of *Pinus sylvestris* needles to light. Tree Physiol 21:1231–1244.

——— 2002*b* Dependence of needle architecture and chemical composition on canopy light availability in three North American *Pinus* species with contrasting needle length. Tree Physiol 22: 747–761.

Niinemets Ü, O Kull 1995 Effects of light availability and tree size on the architecture of assimilative surface in the canopy of *Picea abies*: variation in shoot structure. Tree Physiol 15:791–798.

Niinemets Ü, A Lukjanova 2003 Total foliar area and average leaf age may be more strongly associated with branching frequency than with leaf longevity in temperate conifers. New Phytol 158: 75–89.

Niinemets Ü, A Lukjanova, AD Sparrow, MH Turnbull 2005*a* Light-acclimation of cladode photosynthetic potentials in *Casuarina glauca*: trade-offs between physiological and structural investments. Funct Plant Biol 32:571–582.

Niinemets Ü, L Sack 2006 Structural determinants of leaf light-harvesting capacity and photosynthetic potentials. Pages 385–419 *in* K Esser, UE Lüttge, W Beyschlag, J Murata, eds. Progress in botany, vol 67. Springer, Berlin.

Niinemets Ü, A Sparrow, A Cescatti 2005*b* Light capture efficiency decreases with increasing tree age and size in the southern hemisphere gymnosperm *Agathis australis*. Trees 19:177–190.

Niklas KJ 1991 Biomechanical attributes of the leaves of pine species. Ann Bot 68:253–262.

Nilson T 1971 A theoretical analysis of the frequency of gaps in plant stands. Agric Meteorol 8:25–38.

Pearcy RW, H Muraoka, F Valladares 2005 Crown architecture in sun and shade environments: assessing function and trade-offs with a three-dimensional simulation model. New Phytol 166: 791–800.

Pearcy RW, W Yang 1998 The functional morphology of light capture and carbon gain in the redwood forest understory plant, *Adenocaulon bicolor* Hook. Funct Ecol 12:543–552.

Perry JP Jr 1991 The pines of Mexico and Central America. Timber, Portland, OR.

Platt WJ, GW Evans, SJ Rathbun 1988 The population dynamics of a long-lived conifer (*Pinus palustris*). Am Nat 131:491–525.

Rajendran K, P Devaraj 2004 Biomass and nutrient distribution and their return of *Casuarina equisetifolia* inoculated with biofertilizers in farm land. Biomass Bioenergy 26:235–249.

Richardson DM 1998 Forestry trees as invasive aliens. Conserv Biol 12:18–26.

Richardson DM, PW Rundel 1998 Ecology and biogeography of *Pinus*: an introduction. Pages 3–46 *in* DM Richardson, ed. Ecology and biogeography of *Pinus*. Cambridge University Press, Cambridge.

Ross J 1981 The radiation regime and architecture of plant stands. Junk, The Hague. 342 p.

Shelton MG, MD Cain 2000 Regenerating uneven-aged stands of loblolly and shortleaf pines: the current state of knowledge. For Ecol Manag 129:177–193.

Sokal RR, FJ Rohlf 1995 Biometry: the principles and practice of statistics in biological research. WH Freeman, New York. 887 p.

Sprugel DG, JR Brooks, TM Hinckley 1996 Effects of light on shoot geometry and needle morphology in *Abies amabilis*. Tree Physiol 16:91–98.

Stenberg P, T Kangas, H Smolander, S Linder 1999 Shoot structure, canopy openness, and light interception in Norway spruce. Plant Cell Environ 22:1133–1142.

Stenberg P, S Palmroth, BJ Bond, DG Sprugel, H Smolander 2001 Shoot structure and photosynthetic efficiency along the light gradient in a Scots pine canopy. Tree Physiol 21:805–814.

Stenberg P, H Smolander, DG Sprugel, S Smolander 1998 Shoot structure, light interception, and distribution of nitrogen in an *Abies amabilis* canopy. Tree Physiol 18:759–767.

Takenaka A 1994 Effects of leaf blade narrowness and petiole length on the light capture efficiency of a shoot. Ecol Res 9: 109–114.

ter Steege H 1996 Winphot 5: a programme to analyze vegetation indices, light and light quality from hemispherical photographs. Tropenbos Guayana Reports, 95-2. Tropenbos Guayana Programme, Tropenbos, Georgetown, Guayana. 40 p.

Valladares F 2003 Light heterogeneity and plants: from ecophysiology to species coexistence and biodiversity. Pages 439–471 *in* K Esser, U Lüttge, W Beyschlag, F Hellwig, eds. Progress in botany, vol 64. Springer, Berlin.

Valladares F, FI Pugnaire 1999 Tradeoffs between irradiance capture and avoidance in semi-arid environments assessed with a crown architecture model. Ann Bot 83:459–469.

Valladares F, JB Skillman, RW Pearcy 2002 Convergence in light capture efficiencies among tropical forest understory plants with contrasting crown architectures: a case of morphological compensation. Am J Bot 89:1275–1284.

Valladares F, SJ Wright, E Lasso, K Kitajima, RW Pearcy 2000 Plastic phenotypic response to light of 16 congeneric shrubs from a Panamanian rainforest. Ecology 81:1925–1936.

van Wesenbeeck BK, T van Mourik, JF Duivenvoorden, AM Cleef 2003 Strong effects of a plantation with *Pinus patula* on Andean subpáramo vegetation: a case study from Colombia. Biol Conserv 114:207–218.

Verzino G, P Ingaramo, J Joseau, E Astini, RJ Di, M Dorado 1999 Basal area growth curves for *Pinus patula* in two areas of the Calamuchita Valley, Córdoba, Argentina. For Ecol Manag 124:185–192.

Warren MW, X Zou 2002 Soil macrofauna and litter nutrients in three tropical tree plantations on a disturbed site in Puerto Rico. For Ecol Manag 170:161–171.

Wilson KL, LAS Johnson 1989 Casuarinaceae. Pages 138–174 *in* AS George, ed. Flora of Australia. Vol 3. Hamamelidales to Casuarinales. Australian Government Publishing Service, Canberra.

Yirdaw E, O Luukkanen 2004 Photosynthetically active radiation transmittance of forest plantation canopies in the Ethiopian highlands. For Ecol Manag 188:17–24.